2011

RNAi screening reveals requirement for host cell secretory pathway in infection by diverse families of negative-strand RNA viruses

Debasis Panda
University of Nebraska-Lincoln

Anshuman Das
University of Nebraska-Lincoln, adas2@unl.edu

Phat X. Dinh
University of Nebraska-Lincoln, s-pdinh3@unl.edu

Sakthivel Subramaniam
University of Nebraska-Lincoln

Debasis Nayak
National Institutes of Health

RNAi screening reveals requirement for host cell secretory pathway in infection by diverse families of negative-strand RNA viruses

Debasis Panda[a,b], Anshuman Das[a,b], Phat X. Dinh[a,b], Sakthivel Subramaniam[a,b], Debasis Nayak[c], Nicholas J. Barrows[d], James L. Pearson[d], Jesse Thompson[b], David L. Kelly[e], Istvan Ladunga[f], and Asit K. Pattnaik[a,b,1]

[a]School of Veterinary Medicine and Biomedical Sciences and [b]Nebraska Center for Virology, University of Nebraska, Lincoln, NE 68583; [c]National Institute of Neurological Disorders and Stroke, National Institutes of Health, Bethesda, MD 20892; [d]Duke RNAi Screening Facility, Duke University Medical Center, Durham, NC 27710; [e]University of Nebraska Medical Center, Omaha, NE 68198; and [f]Department of Statistics, University of Nebraska, Lincoln, NE 68588

Edited by Peter Palese, Mount Sinai School of Medicine, New York, NY, and approved October 17, 2011 (received for review August 19, 2011)

Negative-strand (NS) RNA viruses comprise many pathogens that cause serious diseases in humans and animals. Despite their clinical importance, little is known about the host factors required for their infection. Using vesicular stomatitis virus (VSV), a prototypic NS RNA virus in the family *Rhabdoviridae*, we conducted a human genome-wide siRNA screen and identified 72 host genes required for viral infection. Many of these identified genes were also required for infection by two other NS RNA viruses, the lymphocytic choriomeningitis virus of the *Arenaviridae* family and human parainfluenza virus type 3 of the *Paramyxoviridae* family. Genes affecting different stages of VSV infection, such as entry/uncoating, gene expression, and assembly/release, were identified. Depletion of the proteins of the coatomer complex I or its upstream effectors ARF1 or GBF1 led to detection of reduced levels of VSV RNA. Coatomer complex I was also required for infection of lymphocytic choriomeningitis virus and human parainfluenza virus type 3. These results highlight the evolutionarily conserved requirements for gene expression of diverse families of NS RNA viruses and demonstrate the involvement of host cell secretory pathway in the process.

RNA interference | transcription and replication | host cell factors for virus infection

Negative-strand (NS) RNA viruses include a large group of human and animal pathogens that cause diseases ranging from mild flu-like symptoms to fatal hemorrhagic fever. Vesicular stomatitis virus (VSV), the prototype of the family *Rhabdoviridae*, is an enveloped virus with a nonsegmented NS RNA genome. VSV infects most vertebrate and many invertebrate cells and has a short infection cycle. These characteristics have earned appreciation for VSV as an excellent model for understanding virus entry, genome uncoating, replication, assembly, and budding processes, as well as for studying innate and adaptive immune defense mechanisms. VSV is also used as a viral vaccine vector, as an oncolytic agent, and for gene therapy (1).

VSV encodes five proteins: the nucleocapsid protein (N), the phosphoprotein (P), the matrix protein (M), the glycoprotein (G), and the large polymerase protein (L) (2). The viral RNA exists in the virion core as N protein-bound nucleocapsid (NC) to which the viral polymerase is associated. During infection, VSV binds to susceptible cells, although the receptor(s) mediating virus entry remains unidentified (3). It enters cells by clathrin-mediated endocytosis, requiring endocytic adaptor protein AP-2, actin, and dynamin (4–6). Once in the cytoplasm, low pH-dependent fusion of viral envelope with the endosomal membrane leads to the release of NC in the cytoplasm for transcription and replication to occur. Progeny NCs are transported toward the cell periphery in a microtubule-dependent manner (7). Assembly of the viral components occurs at the plasma membrane, and nascent virions are released from the cells.

Viruses use key cellular pathways for their infection and replication (8, 9). Although much is known about the viral proteins in the biology of the virus, little is known about the host factors in VSV and other NS RNA virus infections. Identifying the cellular factors and studying the mechanisms of their involvement in these viral infections is important not only for understanding the biology of these pathogens, but also for development of antiviral therapeutics.

The advent of siRNA technology and the availability of genome-wide siRNA libraries have been useful in identifying host factors required for influenza virus, an NS RNA virus, and several positive-strand RNA viruses, as well as HIV (10–19). The lack of similar studies with other NS RNA viruses has limited the understanding of the role of host cell factors in replication of these viruses. Using VSV, we conducted a genome-wide siRNA screen to identify mammalian genes required for viral infection. Our studies revealed requirements for several cellular pathways and proteins in VSV infection. Many of the factors identified in the screen for VSV are also required for infection by two other NS RNA viruses: the human parainfluenza virus type 3 (HPIV3), a nonsegmented NS RNA virus in the family *Paramyxoviridae*, and the lymphocytic choriomeningitis virus (LCMV), a segmented genome NS RNA virus in the family *Arenaviridae*. Interestingly, for these three viruses representing diverse families of NS RNA viruses, viral gene expression required the function of the coatomer complex I (COPI), a coat protein complex involved in retrograde vesicular transport from the Golgi to the endoplasmic reticulum (ER) (20). Overall, the studies reveal a critical need for the cellular secretory pathway in gene expression of disparate families of NS RNA viruses.

Results

Genome-Wide RNAi Screen for Host Factors in VSV Infection. To identify host proteins required for VSV infection, a genome-wide siRNA screen was conducted. Four independent siRNAs, grouped into a 2 × 2 pool format (Fig. 1*A*), targeting each of 22,909 mammalian genes, were used. VSV-eGFP, a recombinant virus encoding enhanced green fluorescent protein (eGFP) (7), was used to infect HeLa cells. Expression of eGFP in the cells would indicate virus infection and gene expression. AllStars nontargeting (NT) siRNA and siRNAs targeting the VSV L and N mRNAs were used as controls. At 52 h post-siRNA transfection (hpt), cells were infected with VSV-eGFP (hereafter VSV), and at 18 h postinfection (hpi), they were fixed, stained for nuclei, and processed for automated image analysis. Cell number and percent infection were obtained for each well. Infection of NT siRNA-transfected cells was optimized to yield, on average, 60% infection rate. Under these conditions, the rate of infection of cells

Author contributions: D.P. and A.K.P. designed research; D.P., A.D., P.X.D., S.S., N.J.B., and J.T. performed research; D.P., A.D., P.X.D., S.S., D.N., N.J.B., J.L.P., D.L.K., I.L., and A.K.P. analyzed data; and D.P. and A.K.P. wrote the paper.

The authors declare no conflict of interest.

This article is a PNAS Direct Submission.

[1]To whom correspondence should be addressed. E-mail: apattnaik2@unl.edu.

This article contains supporting information online at www.pnas.org/lookup/suppl/doi:10.1073/pnas.1113643108/-/DCSupplemental.

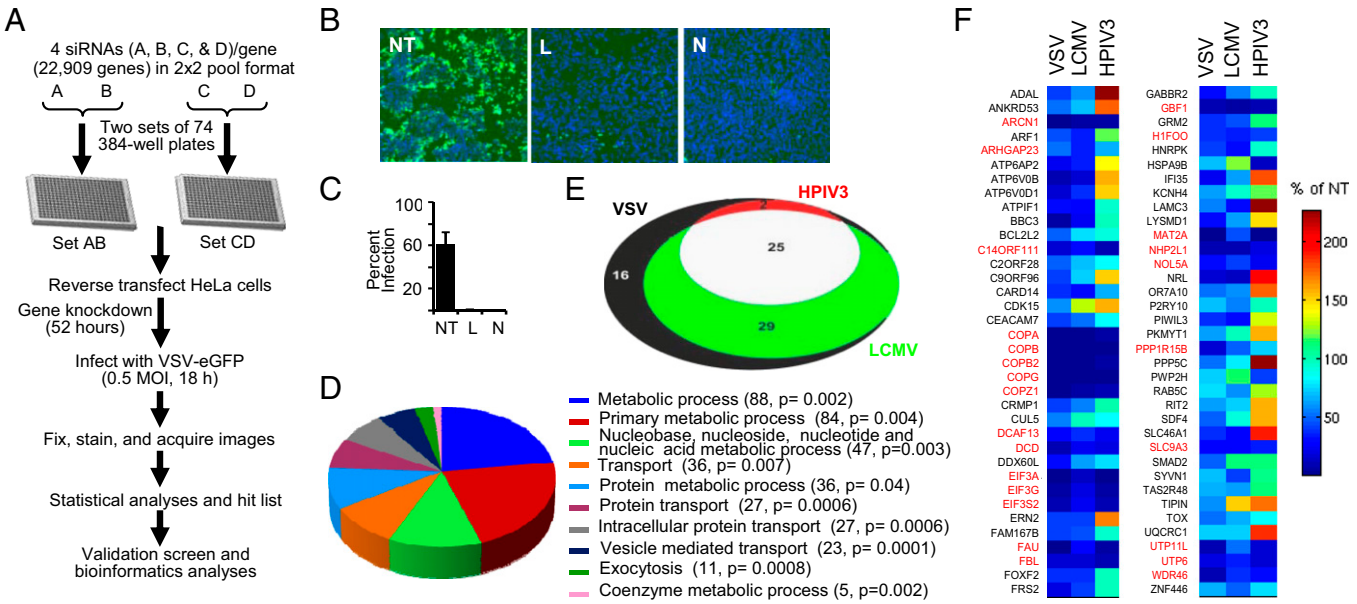

Fig. 1. The RNAi screen. (*A*) Schematic of the RNAi screen. (*B*) Representative images of cells treated with AllStars NT, L, and N siRNAs and infected with VSV-eGFP. (*C*) Bar graph showing the percent infection (mean ± SD) of cells for control siRNAs in the genomic screen. (*D*) Overrepresented *Panther* categories of biological processes of cellular genes identified in the screen. The number of genes in each category and statistical significance (*P*) are shown. (*E*) The extent of overlap among the validated genes for VSV, LCMV, and HPIV3 is shown in the Venn diagram. (*F*) Percent infections for the validated genes normalized to that of NT siRNA are presented as a heat map. Data represents average of four experiments for VSV and two experiments for LCMV and HPIV3. Genes required for all three viruses are shown in red.

transfected with L and N siRNAs was reproducibly <1% (Fig. 1 *B* and *C*). Wells with low cell number due to combined effects of siRNA toxicity and VSV cytopathic effects (*SI Experimental Procedures*) were excluded from further analyses. Sum rank analysis (21) was used, and 233 host genes ($P < 0.01$) were identified as required for VSV infection.

We found several expected genes, including those of the canonical ribosomal proteins, key parts of the cellular translational machinery. We deleted the ribosomal protein genes and narrowed down the list to 173 genes (Dataset S1). Because our screen design used a 2 × 2 siRNA pool format, the 173 genes exhibited the same phenotype with at least two different siRNAs (at least one from each pool), a recommended criterion for true hit identification (22). Thus, the 173 genes identified may represent factors required for VSV infection. The biological process categories of cellular genes overrepresented in the list based on the *Panther* classification system (23) include genes involved in metabolic processes, nucleic acid metabolism, intracellular protein transport, vesicle-mediated transport, and exocytosis, among others (Fig. 1*D*). Pathway analysis revealed that protein functions involved in at least eight major cellular pathways were significantly enriched and showed possible interconnections between these pathways for VSV infection (Fig. S1*A*). Comparison of the mammalian genes identified from genome-wide siRNA screens for other RNA viruses (10–13, 15, 16, 24, 25) with those from the VSV screen revealed that genes in several major biological functions categories are shared by RNA viruses (Fig. S1*B*).

We then conducted a validation screen for the 173 identified genes using siRNAs from another source, Dharmacon ON-TARGETplus pool of four siRNAs. The validation screen was performed in four replicates, and analysis of the results (*SI Experimental Procedures*) led to identification of 72 out of the 173 genes as required for VSV infection (Fig. 1*F* and Dataset S2).

HPIV3 and LCMV Infection Share Many Factors Required for VSV Infection. To identify genes and pathways used by diverse families of NS RNA viruses, the involvement of the 72 genes identified for VSV was examined in HPIV3 and LCMV infection. These viruses belong to distinct families of NS RNA viruses and have common as well as unique strategies for entry, uncoating, replication, and virus assembly. GFPs expressing LCMV and HPIV3 (26, 27) were used, and the screen was conducted as described for VSV in duplicate. By using this strategy, 54 and 27 genes were identified as required for LCMV and HPIV3 infection, respectively, whereas 25 genes were required for infection by all three viruses (Fig. 1*E*). The genes identified for infection by the three viruses along with their known and putative functions, can be found in Datasets S2 and S3, respectively. The normalized percent infection for the 72 genes identified as required for VSV are shown in the heat map (Fig. 1*F*) and are compared with those found for LCMV and HPIV3.

Identification of Genes Involved in Various Stages of VSV Infection. The screen used a multicycle VSV infection assay that included all stages of the virus infection cycle, such as entry and uncoating, transcription and replication, and assembly and release. Our screen identified several subunits of vATPase as necessary for VSV infection (Fig. 1*F* and Fig. S2), confirming the known role of vATPase in endocytosis and virus uncoating (28).

The screen identified several solute carriers localized to the plasma membrane, including the solute carrier family 46 member 1 [SLC46A1; proton-coupled folate transporter (PCFT)]. We examined the role of SLC46A1 in VSV infection. Results showed that in siRNA-treated cells infected with VSV or VSVΔG [a virus that lacks the G gene and cannot produce infectious virus, so the infection with this virus is limited to single cycle only (29)], VSV gene expression (levels of M protein) was reduced (Fig. 2*A*). We then transfected VSV NC to cells treated with siRNAs for SLC46A1 to bypass the endosome-mediated entry and uncoating and examined the effects of depletion of the protein on gene expression. VSV NCs are not infectious per se when added to cells but can initiate the viral genome transcription and replication when delivered into the cytoplasm by transfection. Results show that virus gene expression from transfected NCs remained unaffected (Fig. 2*A*). Multiple siRNAs from two different sources also led to reduced viral gene expression as well as depletion of the SLC46A1 protein (Fig. S3*A*), indicating that the inhibitory effect is specific. Together, these results suggest that SLC46A1 may be required for VSV entry and/or uncoating.

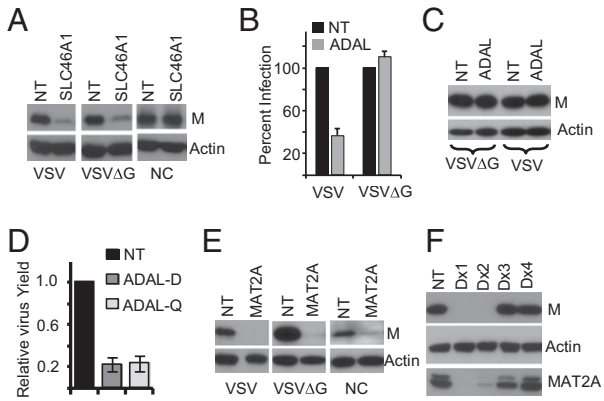

Fig. 2. Identification of genes for VSV entry/uncoating, assembly/budding, and gene expression. (*A*) Cells were transfected with SLC46A1 siRNA for 72 h and infected with viruses (VSV, 0.005 MOI; VSVΔG, 0.2 MOI) or transfected with NC. Cell extracts prepared at 14 hpi (VSV), 5 hpi (VSVΔG), or 6 hpt (NC) were examined for M expression. (*B*) Experiment was performed as in *A* by using ADAL siRNAs, and percent infection was determined. Values are normalized to NT siRNA and represent mean ± SD from three experiments. (*C*) Cells transfected with ADAL siRNA were infected with VSV (0.1 MOI) or VSVΔG (0.2 MOI), and M protein expression was examined at 5 hpi. (*D*) Relative VSV yield (mean ± SD) at 14 hpi (0.001 MOI) after ADAL siRNAs from Dharmacon (ADAL-D) or Qiagen (ADAL-Q) treatment from three experiments. (*E*) Effect of siRNA for MAT2A on viral gene expression in cells infected with VSV or VSVΔG or transfected with NCs. Experimental conditions are as in *A*. (*F*) Cells were transfected with individual siRNA duplexes (Dharmacon) for MAT2A and infected with VSV (0.005 MOI) for 12 h. Cell lysates were examined for levels of M, actin, and MAT2A proteins.

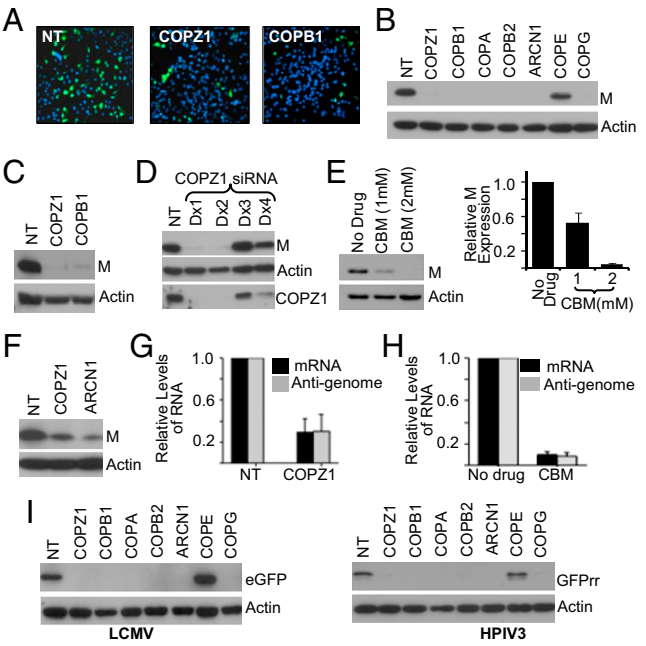

Fig. 3. COPI is required for VSV, LCMV, and HPIV3 infection. (*A*) HeLa cells transfected with siRNAs for COPI subunits were infected with VSV (MOI = 0.01), and at 14 hpi, they were fixed, stained with DAPI, and imaged at 10× magnification. (*B*) Cells transfected with siRNAs for COPI subunits for 48 h were infected with VSV (0.5 MOI) for 4 h. VSV gene expression was assessed by immunoblotting for M. (*C*) Cells transfected with siRNAs for the COPI subunits as above were infected with VSVΔG virus. At 5 hpi, viral gene expression was assessed by immunoblotting for M. (*D*) Cells transfected with individual siRNAs were infected with VSV for 4 h. VSV gene expression (M level) and COPZ1 levels were assessed by immunoblotting. (*E*) Cells pretreated with CBM for 1 h were infected with VSV as in *B*, and viral gene expression was assessed by immunoblotting for M. (*Right*) Histogram shows relative levels of viral gene expression from three experiments. (*F*) VSV NCs were transfected into cells treated with siRNAs for COPZ1 and ARCN1. At 6 h after NC transfection, viral gene expression was examined by immunoblotting for M. (*G*) VSV mRNA and anti-genomic RNA levels in COPZ1-depleted cells, determined by qRT-PCR using primers and probe concentrations shown in Tables S1 and S2 (*SI Experimental Procedures*). Experimental conditions were as in *B*. Values show mean ± SE of measurement (SEM) of duplicate reactions from two experiments after normalizing to NT control. (*H*) Cells infected with VSV as in *B* were treated with 2 mM CBM at 1 hpi. Viral mRNA and anti-genome levels were determined as in *G*. (*I*) Cells transfected with siRNAs for COPI as in *B* were infected with 1 MOI of LCMV for 7 h or HPIV for 14 h. Viral gene expression was assayed by immunoblotting for eGFP or *Renilla reniformis*-GFP (GFPrr).

To identify genes involved in virus assembly and release, we screened the 72 genes using both multicycle (with VSV) and single-cycle (with VSVΔG) infection assays. We found that in ADAL (Adenosine Deaminase Like) siRNA-treated cells infected with VSV, the percent infection was ~threefold less compared with the NT siRNA-treated cells, whereas the percent infection of cells with VSVΔG was similar in both ADAL and NT siRNA-treated cells (Fig. 2*B*). We found no differences in the level of viral gene expression in cells treated with either siRNAs and infected with either VSVΔG or VSV (Fig. 2*C*). However, infectious virus production was reduced in VSV-infected cells treated separately with two different sources of ADAL siRNA (Fig. 2*D*). These results suggest that ADAL may facilitate VSV assembly and/or release.

Further, we found that methionine adenosyltransferase 2A (MAT2A) siRNA treatment reduced VSV gene expression significantly (Fig. 2*E*). MAT2A is involved in L-methionine metabolism and catalyzes formation of *S*-adenosylmethionine (30). MAT2A siRNA treatment also reduced gene expression in cells infected with VSVΔG or in cells transfected with NCs (Fig. 2*E*). Multiple siRNAs for MAT2A led to depletion of the MAT2A protein and corresponding reduction in VSV gene expression (Fig. 2*F*). Viral mRNA and anti-genome levels were reduced in cells treated with MAT2A siRNA (Fig. S3*B*). These results indicate that MAT2A may have a role in viral gene expression.

COPI Is Necessary for VSV Infection at the Level of Viral Gene Expression. Network analysis revealed vesicle trafficking as one of the top scoring pathways required for infection. COPI is involved in retrograde vesicular transport of luminal and membrane proteins from the Golgi to the ER and intra-Golgi transport (20). We focused on COPI because multiple proteins in this pathway were identified and siRNAs for COPI subunits (except COPE) exhibited strong inhibition of VSV infection (Fig. 1*F*). Fig. 3*A* shows inhibition in VSV infection in cells treated with COPZ1 or COPB1 siRNAs.

Because the early secretory pathway is necessary for VSV G protein processing (31), it is possible that the COPI depletion might have affected G protein processing and, consequently, virion assembly and release. To determine whether COPI plays any role in other steps of the VSV infection cycle, we examined the effect of COPI subunit siRNAs on VSV gene expression at 4 hpi, a time at which viral gene expression is readily detectable. At this time, VSV gene expression was inhibited by all COPI siRNAs (except COPE) (Fig. 3*B*). Furthermore, VSVΔG virus infection of cells depleted of COPZ1 and COPB1 showed a significant reduction of viral gene expression (Fig. 3*C*), indicating that COPI plays a role in facilitating viral entry, uncoating, and/or gene expression. The degree of inhibition of VSV gene expression correlated with the level of depletion of COPZ1 (Fig. 3*D*) and COPB1 (Fig. S4*A*). Multiple siRNA for each of the COPI subunits (except COPE) reduced VSV gene expression (Fig. S4*B*). We then used 1,3-cyclohexanebismethylamine (CBM), an inhibitor of COPI function (32, 33), to examine involvement of COPI in VSV gene expression. Treatment of cells with CBM 1 h before infection reduced VSV M protein levels in a dose-dependent manner (Fig. 3*E*) without adversely affecting the cell viability (Fig. S5). These studies suggest that COPI is necessary for VSV infection.

Since COPI is involved in endosomal transport (34), it is possible that the inhibition of VSV gene expression could be due to disruption of endosomal transport required for VSV entry and uncoating. However, inhibition of viral gene expression was observed in NC-transfected cells depleted of COPI subunits (Fig. 3*F*), suggesting that COPI is required for viral gene expression, independent of entry and uncoating steps. Additionally, we found reduced levels of mRNA (transcription product) and anti-genome (replication product) in COPZ1-depleted cells (Fig. 3*G*). Furthermore, when cells were treated with CBM 1 h after VSV infection, a time-frame in which the majority of the virus would have uncoated their NCs (35), reduced levels of mRNA and anti-genome were also observed (Fig. 3*H*), suggesting that COPI is required for VSV gene expression.

We then examined whether COPI is also required for gene expression of LCMV and HPIV3. Cells treated with siRNA for COPI subunits were infected with GFP-encoding LCMV or HPIV3. The level of GFP protein was examined in cell extracts collected at the earliest time point when GFP expression was seen in infected cells (7 hpi for LCMV or 14 hpi for HPIV3) (26). Depletion of the COPI subunits (except COPE) significantly inhibited LCMV and HPIV3 gene expression (Fig. 3*I*), suggesting that these viruses also require COPI functions.

Viral Gene Expression Requires ARF1 and GBF1, the Upstream Effectors of COPI. Activation of ADP ribosylation factor 1 (ARF1) is required for the recruitment of COPI complex onto the Golgi membranes (36). In ARF1 siRNA-treated cells infected with VSV, the viral gene expression was reduced by twofold with concomitant similar reduction in the levels of ARF1 protein (Fig. 4*A* and Fig. S6*A*), suggesting that moderate inhibition of viral gene expression may be due to insufficient depletion of ARF1. In cells transfected with a plasmid encoding a dominant-negative mutant, ARF1-T31N (37), viral gene expression was inhibited (Fig. 4*B*). ARF1 depletion also inhibited LCMV gene expression but surprisingly had no effect on HPIV3 gene expression (Fig. 4*C*). It is possible that moderate level of ARF1 depletion might not have shown measurable inhibitory effect on HPIV3 gene expression.

The Golgi-associated brefeldin A resistant factor 1 (GBF1) is the guanine nucleotide exchange factor, which catalyzes GDP–GTP exchange to activate ARF1 for COPI recruitment onto the Golgi membranes (38). GBF1 siRNA reduced endogenous GBF1 protein levels by >90% and led to significant reduction in VSV M protein (Fig. 4*D*). Reduction in VSV mRNA and anti-genome levels was observed after GBF1 depletion (Fig. S6*B*), suggesting that VSV gene expression requires GBF1.

We then used inhibitors of GBF1 to probe its requirement in VSV gene expression. Brefeldin A (BFA) inhibits GBF1, BIG1 (brefeldin-inhibited guanine nucleotide exchange factor 1), and BIG2, whereas Golgicide A (GCA) and Tyrphostin AG1478 are specific inhibitors of GBF1 (39, 40). In the presence of these drugs, VSV gene expression was inhibited (Fig. 4 *E* and *F*). The drugs had no significant adverse effects on viability of uninfected cells (Fig. S5). We then examined VSV gene expression in Madin Darby canine kidney (MDCK) cells, which contain a natural mutation (M832L) in GBF1, rendering the cells resistant to BFA, GCA, and AG1478 (39–41). However, in these cells, BIG1 and BIG2 are sensitive to BFA (40). In MDCK cells infected with VSV, viral gene expression was not adversely affected, even at higher concentrations of the drugs (Fig. S6*C*). Studies with VSVΔG virus infection (Fig. S6*D*) and NC transfection (Fig. S6*E*) showed that GBF1 is required for VSV gene expression. In LCMV and HPIV3 infected cells, viral gene expression was reduced after depletion of GBF1 (Fig. 4*G*) and was sensitive to GBF1 inhibitors (Fig. 4 *H* and *I*), indicating that GBF1 is also required for these viruses.

Discussion

In the present study, using a genome-wide siRNA screen, we have identified host cell factors required for VSV infection. Because of our screen design (2 × 2 pool of siRNA format) and validation using a different source of siRNAs, the possibility of false positives in the list is likely to be low, but it may have compromised our ability to identify additional genes required for VSV infection. An integrated model (Fig. 5) revealing the host factors required for VSV infection demonstrates many previously undescribed functions and pathways used not only by VSV but also by other RNA viruses such as LCMV and HPIV3. This study provides a comparative analysis of cellular factors involved in replication of three disparate NS RNA viruses. Functions such as RNA processing, vesicular transport, transcription, and translation regulations, among others, are shared by all three viruses, which would suggest utilization of common cellular functions for their replication. It should be noted that the factors identified for LCMV and HPIV3 are only a subset of those identified for VSV and do not represent a complete set of factors required for either LCMV or HPIV3. However, it is evident that several of the cellular pathways and factors are shared by all three viruses, illustrating commonalities in the requirements for replication of these NS RNA viruses.

Although VSV is phylogenetically more closely related to HPIV3 than LCMV (42), only 27 of the 72 factors identified for VSV were required for HPIV3, whereas 54 of those were required

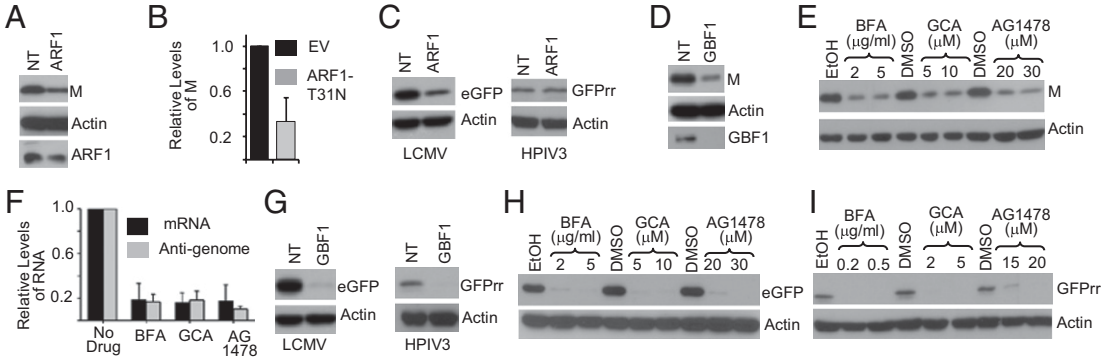

Fig. 4. Viral gene expression requires ARF1 and GBF1. (*A*) Cells transfected with ARF1 siRNAs for 72 h were infected with VSV (0.05 MOI). M protein and ARF1 expression were examined at 6 hpi by immunoblotting. (*B*) Cells were transfected with empty vector (EV) or ARF1-T31N encoding vector. At 24 hpt, cells were infected with VSV (0.5 MOI) for 4 h. M protein levels from three experiments are shown as mean ± SD. (*C*) Cells transfected with ARF1 siRNAs were infected with LCMV or HPIV3 (as in Fig. 3*I*). Viral gene expression was examined by immunoblotting for eGFP or GFPrr. (*D*) Cells transfected with GBF1 siRNAs for 72 h were infected with VSV (0.5 MOI) for 4 h. M and GBF1 were examined by immunoblotting. (*E*) Cells infected with VSV (1 MOI) were treated with the drugs at 1 hpi. Cell lysates at 4 hpi were assessed for M. (*F*) Cells infected with VSV were treated with BFA (2 μg/mL), GCA (10 μM), and AG1478 (30 μM) at 1 hpi for 2 h. Fold change in mRNA and anti-genome levels were determined as in Fig. 3*H*. Mean ± SEM ($n = 2$) is shown. (G) GBF1 siRNA transfected cells were infected with LCMV or HPIV3, and viral gene expression was measured as described in Fig. 3*I*. (*H* and *I*) Cells infected with 1 MOI of LCMV (*H*) or HPIV3 (*I*) were treated at 1 hpi with the drugs. Viral gene expression was assessed by immunoblotting for eGFP or GFPrr at 7 (LCMV) or 14 (HPIV3) hpi.

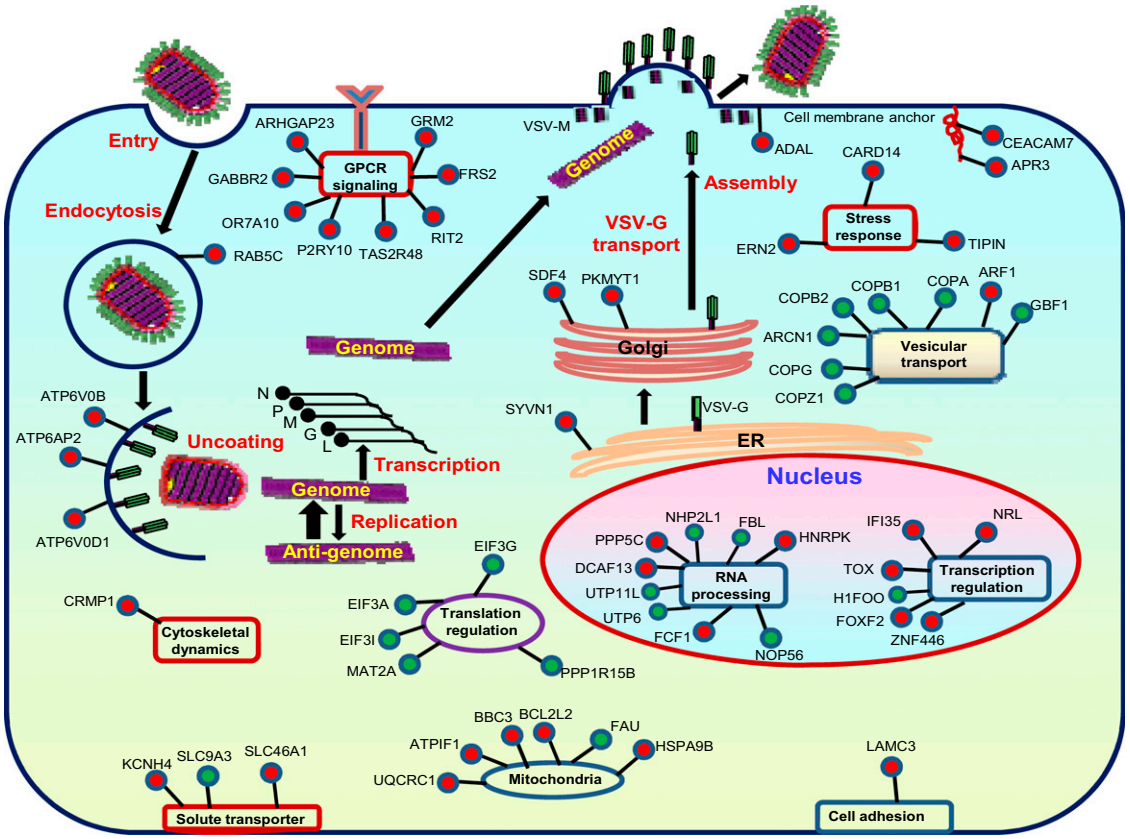

Fig. 5. Integrated model of host factors required for VSV, LCMV, and HPIV3. Genes were placed at positions most likely relevant to VSV infection. Subcellular localization and biological functions of the proteins were determined by using Entrez Gene, Entrez PubMed, and UniProt. Genes shown as green circles are shared by all three viruses, whereas genes shown as red circles are either for VSV only or shared by VSV and LCMV or by VSV and HPIV3.

for LCMV. We noted an enrichment of proteins involved in GPCR signaling, indicating that signaling through some of these GPCR components may be required for infection. The observations that SLC46A1 (PCFT) is specifically required in entry/uncoating, ADAL is required for assembly/budding, and MAT2A is required for gene expression of VSV are unique findings of this study. ADAL was recently discovered as a putative plasma membrane protein closely related to adenosine deaminase with unknown function. Further studies are required for understanding the molecular mechanisms of its involvement in VSV infection. Identification of MAT2A, in VSV RNA synthesis, suggests its possible involvement in VSV mRNA cap formation during transcription. Whether these identified proteins are directly involved in various steps in VSV infection or whether they mediate their activities through other cellular interacting partners (Fig. S7) is of interest for a mechanistic understanding of their role in VSV infection.

The subunits of COPI complex emerged strongly as factors required for infection by all three viruses. The heptameric COPI complex associates with the Golgi membranes, resulting in the budding of COPI-containing vesicles, whose major function is to mediate transport of cellular proteins and cargo from the Golgi to the ER as well as the intra-Golgi transport (20). Depletion of COPI also perturbs the steady-state distribution of the Golgi enzymes (43) and thus inhibits processing of the VSV G protein and its transport to the plasma membrane (44, 45). Further, we have found that depletion of COPZ1 subunit had no adverse effect on VSV G protein-mediated entry of pseudotyped HIV (Fig. S8), consistent with recent studies that BFA has no significant effect on VSV G-mediated entry of retrovirus (46). The following observations suggest that COPI is involved in VSV gene expression: (*i*) VSV gene expression is inhibited in COPI-depleted cells that are independent of the viral G protein processing, (*ii*) pharmacologic inhibitor of COPI inhibits VSV gene expression as well as viral RNA levels, and (*iii*) VSV gene expression is reduced in NC transfected cells that have been depleted of COPI.

Multiple siRNA screens for influenza virus, an NS RNA virus that replicates in the nucleus, have identified COPI, but not COPII, as required for infection (11, 12, 24). Although COPI is required for influenza as well as VSV G-mediated virus entry (12), our results for VSV are in contrast to these studies. It is possible that the assay conditions, cell type used, and other unknown factors may have contributed to these disparate results. In this report and also in earlier reports (11, 15, 47), the siRNA for COPE did not inhibit VSV and other virus infections, indicating that this protein may not have been depleted sufficiently to observe the effect or that COPE may be dispensable for COPI function in viral infection (11, 15, 47). Transfection of siRNAs for COPII subunits resulted in statistically nonsignificant reduction of VSV infection (Fig. S9), indicating that COPII may not be required for VSV, consistent with the result that it was also not identified in the influenza virus screens (11, 12, 24). Our results point toward a specific role of COPI in VSV gene expression. The requirement for ARF1 and GBF1, the upstream activators of COPI assembly in modulating VSV RNA levels, suggests a role for the host cell secretory pathway in the process. Whether the COPI complex is directly involved in regulating the viral polymerase functions or whether it may signal through downstream effectors required for viral gene expression is of further interest.

The requirement of COPI for genome replication has been well documented for positive-strand RNA viruses, which replicate in association with cytoplasmic membranous structures (9, 15, 47). Viruses such as polio, hepatitis C, and coxsackie modulate the activities of ARF1, GBF1, and COPI for formation of intracellular organelles for replication (48, 49). Vaccinia virus, a DNA virus,

requires COPI for its biogenesis, whereas HIV lacks a requirement for COPI (33). The studies presented here reveal a requirement for COPI in gene expression of VSV, and possibly other NS RNA viruses, suggesting a critical role of this secretory pathway in RNA virus infection. Most NS RNA viruses including VSV, LCMV, and HPIV3, replicate in the cytoplasm. The replication organelles, if any, for the cytoplasmically replicating NS RNA viruses are unknown. VSV replicates throughout the cytoplasm of infected cells (7, 50), although studies do not rule out the existence of specific replication organelles in the cytoplasm. Further biochemical and ultrastructural studies in cells infected with VSV and other NS RNA viruses will likely illuminate the nature of the replication organelles for these viruses.

In conclusion, this study has identified several previously undescribed candidates and pathways regulating infection of cells by VSV and two other NS RNA viruses. The requirement for host cell secretory pathway in infection by VSV, LCMV, and HPIV3 argues for a common mechanism by which this cellular pathway modulates NS RNA virus replication.

Experimental Procedures

The high-throughput primary siRNA screen was performed by using the Qiagen genome-wide siRNA library (Version 1.0). The validation screen was conducted by using Dharmacon ON-TARGETplus pool of four siRNAs. Details of the screen design, statistical analysis, hit identification, and other experimental procedures can be found in *SI Experimental Procedures*.

ACKNOWLEDGMENTS. We thank G. Belov, P. Collins, J. Donaldson, D. Lyles, D. McGavern, and E. Sztul for reagents and Z. H. Gill for excellent assistance in the laboratory. The work was supported in part by National Institutes of Health Grant R01AI34956.

1. Barber GN (2005) VSV-tumor selective replication and protein translation. *Oncogene* 24:7710–7719.
2. Barr JN, Whelan SP, Wertz GW (2002) Transcriptional control of the RNA-dependent RNA polymerase of vesicular stomatitis virus. *Biochim Biophys Acta* 1577:337–353.
3. Coil DA, Miller AD (2004) Phosphatidylserine is not the cell surface receptor for vesicular stomatitis virus. *J Virol* 78:10920–10926.
4. Johannsdottir HK, Mancini R, Kartenbeck J, Amato L, Helenius A (2009) Host cell factors and functions involved in vesicular stomatitis virus entry. *J Virol* 83:440–453.
5. Cureton DK, Massol RH, Saffarian S, Kirchhausen TL, Whelan SP (2009) Vesicular stomatitis virus enters cells through vesicles incompletely coated with clathrin that depend upon actin for internalization. *PLoS Pathog* 5:e1000394.
6. Sun X, Yau VK, Briggs BJ, Whittaker GR (2005) Role of clathrin-mediated endocytosis during vesicular stomatitis virus entry into host cells. *Virology* 338:53–60.
7. Das SC, Nayak D, Zhou Y, Pattnaik AK (2006) Visualization of intracellular transport of vesicular stomatitis virus nucleocapsids in living cells. *J Virol* 80:6368–6377.
8. Watanabe T, Watanabe S, Kawaoka Y (2010) Cellular networks involved in the influenza virus life cycle. *Cell Host Microbe* 7:427–439.
9. Miller S, Krijnse-Locker J (2008) Modification of intracellular membrane structures for virus replication. *Nat Rev Microbiol* 6:363–374.
10. Brass AL, et al. (2008) Identification of host proteins required for HIV infection through a functional genomic screen. *Science* 319:921–926.
11. Brass AL, et al. (2009) The IFITM proteins mediate cellular resistance to influenza A H1N1 virus, West Nile virus, and dengue virus. *Cell* 139:1243–1254.
12. König R, et al. (2010) Human host factors required for influenza virus replication. *Nature* 463:813–817.
13. Krishnan MN, et al. (2008) RNA interference screen for human genes associated with West Nile virus infection. *Nature* 455:242–245.
14. Sessions OM, et al. (2009) Discovery of insect and human dengue virus host factors. *Nature* 458:1047–1050.
15. Tai AW, et al. (2009) A functional genomic screen identifies cellular cofactors of hepatitis C virus replication. *Cell Host Microbe* 5:298–307.
16. Li Q, et al. (2009) A genome-wide genetic screen for host factors required for hepatitis C virus propagation. *Proc Natl Acad Sci USA* 106:16410–16415.
17. Hao L, et al. (2008) Drosophila RNAi screen identifies host genes important for influenza virus replication. *Nature* 454:890–893.
18. Cherry S, et al. (2005) Genome-wide RNAi screen reveals a specific sensitivity of IRES-containing RNA viruses to host translation inhibition. *Genes Dev* 19:445–452.
19. König R, et al. (2008) Global analysis of host-pathogen interactions that regulate early-stage HIV-1 replication. *Cell* 135:49–60.
20. Lippincott-Schwartz J, Liu W (2006) Insights into COPI coat assembly and function in living cells. *Trends Cell Biol* 16:e1–e4.
21. Barrows NJ, Le Sommer C, Garcia-Blanco MA, Pearson JL (2010) Factors affecting reproducibility between genome-scale siRNA-based screens. *J Biomol Screen* 15: 735–747.
22. Echeverri CJ, et al. (2006) Minimizing the risk of reporting false positives in large-scale RNAi screens. *Nat Methods* 3:777–779.
23. Thomas PD, et al. (2003) PANTHER: a library of protein families and subfamilies indexed by function. *Genome Res* 13:2129–2141.
24. Karlas A, et al. (2010) Genome-wide RNAi screen identifies human host factors crucial for influenza virus replication. *Nature* 463:818–822.
25. Zhou H, et al. (2008) Genome-scale RNAi screen for host factors required for HIV replication. *Cell Host Microbe* 4:495–504.
26. Emonet SF, Garidou L, McGavern DB, de la Torre JC (2009) Generation of recombinant lymphocytic choriomeningitis viruses with trisegmented genomes stably expressing two additional genes of interest. *Proc Natl Acad Sci USA* 106:3473–3478.
27. Zhang L, et al. (2005) Infection of ciliated cells by human parainfluenza virus type 3 in an in vitro model of human airway epithelium. *J Virol* 79:1113–1124.
28. Luyet PP, Falguières T, Pons V, Pattnaik AK, Gruenberg J (2008) The ESCRT-I subunit TSG101 controls endosome-to-cytosol release of viral RNA. *Traffic* 9:2279–2290.
29. Dinh PX, Beura LK, Panda D, Das A, Pattnaik AK (2011) Antagonistic effects of cellular poly(C) binding proteins on vesicular stomatitis virus gene expression. *J Virol* 85: 9459–9471.
30. Martínez-Chantar ML, et al. (2003) L-methionine availability regulates expression of the methionine adenosyltransferase 2A gene in human hepatocarcinoma cells: Role of S-adenosylmethionine. *J Biol Chem* 278:19885–19890.
31. Orci L, et al. (1997) Bidirectional transport by distinct populations of COPI-coated vesicles. *Cell* 90:335–349.
32. Hu T, Kao CY, Hudson RT, Chen A, Draper RK (1999) Inhibition of secretion by 1,3-Cyclohexanebis(methylamine), a dibasic compound that interferes with coatomer function. *Mol Biol Cell* 10:921–933.
33. Zhang L, et al. (2009) A role for the host coatomer and KDEL receptor in early vaccinia biogenesis. *Proc Natl Acad Sci USA* 106:163–168.
34. Whitney JA, Gomez M, Sheff D, Kreis TE, Mellman I (1995) Cytoplasmic coat proteins involved in endosome function. *Cell* 83:703–713.
35. Das SC, Panda D, Nayak D, Pattnaik AK (2009) Biarsenical labeling of vesicular stomatitis virus encoding tetracysteine-tagged m protein allows dynamic imaging of m protein and virus uncoating in infected cells. *J Virol* 83:2611–2622.
36. Hsu VW, Yang JS (2009) Mechanisms of COPI vesicle formation. *FEBS Lett* 583: 3758–3763.
37. Peters PJ, et al. (1995) Overexpression of wild-type and mutant ARF1 and ARF6: Distinct perturbations of nonoverlapping membrane compartments. *J Cell Biol* 128: 1003–1017.
38. García-Mata R, Szul T, Alvarez C, Sztul E (2003) ADP-ribosylation factor/COPI-dependent events at the endoplasmic reticulum-Golgi interface are regulated by the guanine nucleotide exchange factor GBF1. *Mol Biol Cell* 14:2250–2261.
39. Pan H, et al. (2008) A novel small molecule regulator of guanine nucleotide exchange activity of the ADP-ribosylation factor and golgi membrane trafficking. *J Biol Chem* 283:31087–31096.
40. Sáenz JB, et al. (2009) Golgicide A reveals essential roles for GBF1 in Golgi assembly and function. *Nat Chem Biol* 5:157–165.
41. Lanke KH, et al. (2009) GBF1, a guanine nucleotide exchange factor for Arf, is crucial for coxsackievirus B3 RNA replication. *J Virol* 83:11940–11949.
42. Fauquet CM, Mayo MA, Maniloff J, Desselberger U, Ball LA (2005) In *Virus Taxonomy*. Eighth report of the international committee on the taxonomy of viruses (Elsevier/ Academic Press, London).
43. Tu L, Tai WC, Chen L, Banfield DK (2008) Signal-mediated dynamic retention of glycosyltransferases in the Golgi. *Science* 321:404–407.
44. Szul T, et al. (2007) Dissecting the role of the ARF guanine nucleotide exchange factor GBF1 in Golgi biogenesis and protein trafficking. *J Cell Sci* 120:3929–3940.
45. Manolea F, Claude A, Chun J, Rosas J, Melançon P (2008) Distinct functions for Arf guanine nucleotide exchange factors at the Golgi complex: GBF1 and BIGs are required for assembly and maintenance of the Golgi stack and trans-Golgi network, respectively. *Mol Biol Cell* 19:523–535.
46. Goueslain L, et al. (2010) Identification of GBF1 as a cellular factor required for hepatitis C virus RNA replication. *J Virol* 84:773–787.
47. Cherry S, et al. (2006) COPI activity coupled with fatty acid biosynthesis is required for viral replication. *PLoS Pathog* 2:e102.
48. Belov GA, Feng Q, Nikovics K, Jackson CL, Ehrenfeld E (2008) A critical role of a cellular membrane traffic protein in poliovirus RNA replication. *PLoS Pathog* 4:e1000216.
49. Hsu NY, et al. (2010) Viral reorganization of the secretory pathway generates distinct organelles for RNA replication. *Cell* 141:799–811.
50. Heinrich BS, Cureton DK, Rahmeh AA, Whelan SP (2010) Protein expression redirects vesicular stomatitis virus RNA synthesis to cytoplasmic inclusions. *PLoS Pathog* 6: e1000958.

Supporting Information

Panda et al. 10.1073/pnas.1113643108

SI Experimental Procedures

Cells, Viruses, Virus Infections, and Virus Yield Determination. HeLa (ATCC # CCL2), MDCK, and TZM-bl cells were maintained in DMEM supplemented with 10% FBS and antibiotics. BHK-21 cells were maintained in MEM with 5% FBS. LCMVr3-GFP (1) and HPIV3-GFP (2) were grown in BHK-21 cells and titrated in HeLa cells by fluorescent focus forming assay. Clonal stock of VSV-eGFP was prepared by growing the virus in BHK-21 cells and titrating in HeLa cells by plaque assay. VSV-PeGFPΔG virus has been described (3). VSV yield was determined by plaque assay on HeLa cells.

Antibodies. Anti-M (23H12) monoclonal antibody was from Douglas Lyles (Wake Forest University, Winston-Salem, NC). Anti-actin, anti-eGFP, and anti-*Renilla reniformis*-GFP (GFPrr) antibodies were from Santa Cruz; anti-βCOP, anti-ζCOP, anti-ARF1, and MAT2A antibodies were from Sigma; anti-GBF1 antibody was from BD Science; and anti-SLC46A1 antibody was from Abcam.

SDS/PAGE, Immunoblotting, and Quantitation. These procedures are described (3). Quantitation of proteins detected in the blots was performed by using Versadoc QuantityOne software (BioRad Laboratories).

NC Preparation and Transfection. VSV-eGFP NCs were prepared, and transfection was performed by using Lipofectamine 2000 as described (3).

RNAi Screen. The primary screen was performed at the Duke University RNAi screening facility by using the Qiagen genomic siRNA library v 1.0 consisting of four distinct siRNAs (A, B, C, and D) targeting 22,909 known and putative human genes. The four siRNAs were grouped into two pools, with each pool containing two siRNAs (set AB and set CD). This format resulted in seventy-four 384-well plates per set and a total of 148 plates for the entire screen. This 2 × 2 pool design allowed each gene to be tested by two independent siRNA sets. AllStars nontargeting (NT) siRNA (Qiagen) was used as a negative control. Also, siRNAs targeting N and L genes (two per gene) of VSV were synthesized and used as additional positive control siRNAs. The sequences of the siRNAs targeting the VSV genes are as follows. N1: 5′-CUGCAAGGCCUAAGAGAGA-3′; N2: 5′-UGGAAUACCCGGCAGAUUA-3′; L1: 5′-GCAGUUAUCCAGCAAUCAU-3′; and L2: 5′-GAGAAACGUUGUAGAAUUA-3′.

Corning 384-well tissue culture plates were prearrayed with 1 pmol of siRNA per well by using the Velocity Bravo liquid handling system (Agilent Technologies). Each plate was also seeded with siRNAs targeting VSV N and L gene as well as the NT siRNA. Lipofectamine RNAiMAX (Invitrogen) was used in the amount of 0.05 μL per well in 10 μL of OptiMEM (Invitrogen). Reverse transfection of 3,000 HeLa cells was performed with 15.4 nM final concentration of siRNAs in a 65 μL of total volume. VSV-eGFP virus (grown in BHK-21 cells and titrated in HeLa cells) was used. Initial studies of siRNA transfections (48 and 72 hpt), virus infections at different MOIs (0.2, 0.4, 0.5, 0.6, 0.8, 1, 2, and 3 MOI), and for various lengths of time postinfection (8, 10, 12, 14, 16, and 18 h) were conducted to identify suitable conditions for primary high-throughput screen. To identify factors involved in all stages of the VSV life cycle, such as entry and uncoating, replication, and budding and release, the screen was optimized for MOI and time to allow multiple rounds of virus infection to occur. As a quality control metrics for the assay, Z′ factor (4) was calculated between NT siRNA treated wells and N and L siRNA treated cells. The multiplicity and time of infection was optimized to obtain a Z′ factor value of >0.5, which would indicate a robust assay. Based on these initial standardization experiments, the genome-wide screen was performed by using 0.5 MOI of VSV and 18 h of infection. In the genomic screen, the Z′ factor between NT and L was calculated to be 0.44 for AB set and 0.51 for CD set. These Z′ factor values indicated that we would be able to distinguish the positive control wells (L and N siRNA treated cells) from control NT siRNA treated wells in both AB pool and CD pool.

Automated Image Analysis. At the end of the infection, cells were fixed with 4% paraformaldehyde in PBS, permeabilized with 0.1% Triton X-100 in PBS, and stained with Hoechst 33342 in PBS for 30 min. Stained cells were imaged with a Cellomics ArrayScan VTI automated microscope. Images were analyzed with vHCS Scan Target Activation software v 5.1.2 to identify infected cells. Cells without VSV-eGFP infection served as reference population for background fluorescence. Four fields per well of a 384-well plate were imaged at 10× magnification. First, cells were identified by their nuclei staining in channel 1 of Cellomics. Cells that scored positive in channel 1 were analyzed for GFP expression in channel 2, and GFP intensity was calculated for the cells. Frequency distribution of GFP intensity was plotted and compared between NT siRNA transfected controls infected with VSV-eGFP or uninfected reference population. For selection of infected cells, threshold was set by manual inspection of representative images from VSV-eGFP infected and uninfected cells. Cells appearing at least 5 SDs away from the average intensity of uninfected control population in the same plate or same batch were considered positive for GFP expression. Once the threshold was determined, all of the plates were subjected to data analysis by vHCS Target activation software. Finally, data were obtained by using vHCS View software v 5.1.2, and the numbers of cells present in the well were identified as "Valid Object Count" (VOC), whereas the percentage of infection was determined as "% selected."

Statistical Analysis. Transfection of siRNAs and subsequent infection with VSV resulted in reduced cell number for some wells due to the combined effects of siRNA toxicity, loss of cell survival factors, and VSV cytopathogenicity. We used a cutoff value of 800 or more cell number in four fields per well for further analysis. This criterion requires that wells transfected with siRNA sets AB and CD for a particular gene should have a VOC of at least 800. Using this criterion, we discarded ~24% of the genes in the library. Because our screen was designed to identify factors whose depletion would reduce VSV infection, the genes discarded from further analysis due to reduced cell numbers may potentially represent restriction factors and/or factors required for cell survival. In other words, if a gene is required for VSV infection, its depletion would reduce VSV replication and thus would not promote VSV-mediated cell death. We would then expect to observe higher cell number in those wells. So, rationally, the remaining 76% of the genes in the library should include factors required for VSV replication.

In the screen, for both AB set and CD set, we did not observe a correlation between percent infection and cell number [r (correlation coefficient) = 0.308 (for AB set) and 0.295 (for CD set)]. It has been reported that cell density may impact clathrin-mediated endocytosis and may subsequently affect virus infection (5). However, throughout the primary screen, we used a cell density (3,000 plated cells per well) and MOI (0.5) as well as time (18 hpi)

conditions in which the rate of infection remained in the linear range. The distribution of percent infection for genomic population for the AB and CD pools did not follow a normal distribution, and thus parametric tests would not have given meaningful results. Therefore, we used a nonparametric analysis, the Sum rank statistics (6), to identify the hits from the primary screen. Because of day-to-day variation in percent infection of NT control population, we decided to use batch-wise analysis to get the primary hits. Percent infection values for set AB and set CD were ranked independently from lowest to highest and given ranks from 1 to n (n = the number of samples analyzed), respectively. Sum rank for a particular gene is the sum of rank in AB set and rank in CD set for that gene. The P value for each gene was then determined, and finally samples were aligned according to the P value. A total of 233 genes with $P < 0.01$ were identified as primary candidate hits.

Validation Screen. The validation screen was conducted at the Eppley Institute for Cancer Research at the University of Nebraska Medical College (UNMC) by using Dharmacon ON-TARGETplus pool of four siRNA. The sequences of Dharmacon siRNAs did not overlap with those of Qiagen siRNAs, allowing us to test multiple siRNA. The assay was conducted by using 96-well plates. Six microliters of pooled siRNA (500 nM) was prearrayed per well in 96-well plates by using the Biomek FX liquid handling system. Lipofectamine RNAiMAX and OptiMEM mix was prepared (0.25 μL of LipofectamineRNAiMAX in 20 μL of OptiMEM per well). For experiments using VSV, 15,000 cells in 75 μL of DMEM with 10% FBS and 1× PKS per well were added to each well to yield a final concentration of 30 nM siRNAs. For LCMV and HPIV infection, 10,000 cells per well were added in 75 μL of above medium. Cells were incubated for 50 h for knockdown of the genes. For VSV-eGFP infection, 0.05 MOI of virus was added in 100 μL of DMEM 2% FBS and 1× PKS per well by using a multichannel pipette. LCMVr3-GFP (0.05 MOI) and HPIV3-GFP (0.2 MOI) were used to infect HeLa cells. Virus inoculum containing required MOI of viruses were prepared in 40 μL of DMEM (with 5% FBS and PKS) per well. After 1 h of infection, 60 μL of DMEM with 5% FBS and 1× PKS was added to each well. Cells were infected with VSV for 14 h, with LCMV for 36 h, or with HPIV3 for 41 h. Infected cells were fixed as per the protocol described in the primary screen. Cells were stained with DAPI to stain the nuclei. Image analysis was performed in Cellomics ArrayScan VTI at UNMC to obtain the VOC and percent infection. Experiment was repeated four times for VSV and two times each for LCMV and HPIV3. Meaningful between-plate comparisons required normalization due to variations among plates. Therefore, we normalized the percent infection values by plate-wise medians, separately for siRNA-treated and untreated control samples. We applied the nonparametric Wilcoxon-Mann-Whitney (WMW) rank-sum test (7). Despite the lower statistical power of the nonparametric tests compared with the parametric tests, the WMW test indicated significant effects of the siRNA treatment in the majority of genes compared with untreated controls at the $P \leq 0.01$ level. Normalization was performed by in-house PERL and MATLAB programs. The WMW tests, heat map representations, and other graphics were carried out in MATLAB.

siRNA Transfection in 12-Well Plate. Reverse transfection of HeLa cell was performed in 12-well tissue culture plates. Final concentrations of siRNAs were 20 nM, except for COPI where 10 nM concentrations of siRNAs were used. Required amount of siRNAs were plated in the wells. Lipofectamine RNAiMAX in OptiMEM was prepared (2 μL of Lipofectamine in 300 μL of OptiMEM per well) and added to the wells. Plates were incubated for 30 min for complex formation. HeLa cells (200,000 cells per well in 500 μL of DMEM 10% FBS+ PKS) were added for COPI experiments. For other siRNA transfection experiments, 100,000 cells were added. Cells were further incubated for 42–44 h for COPI siRNAs and 66–68 h for other siRNA transfection. All of the experiments were conducted with Dharmacon ON-TARGET-plus siRNAs, except that where indicated, the Qiagen siRNAs were used.

Quantitative RT-PCR (qRT-PCR). qRT-PCR was used to measure the VSV P mRNA, genome, and anti-genome levels. Total RNA was extracted from cells by TRIzol according to manufacturer's protocol (Invitrogen). First-strand cDNA was synthesized from 200 ng of total RNA by using M-MLV reverse transcriptase according to manufacturer's protocol (Invitrogen). For quantification of P mRNA and the internal control β-actin mRNA, oligo-(dT) was used as primer in one RT reaction. For quantification of anti-genome and the internal control β-actin mRNA, VSV2955R and β-actin1 R (each 2 pmol) were used as primers in another RT reaction. These cDNAs were used as templates in qRT-PCR reactions that were carried out in Cepheid Smart Cycler. The sequences and optimized concentrations of the primers and probes are listed in Tables S1 and S2, respectively. Lightcycler 480 probe master mix (Roche Applied Sciences) was used in qRT-PCR reactions. The thermal setup conditions used included initial denaturation at 95 °C for 5 min, denaturation at 95 °C for 30 s, and annealing and extension at 60 °C for 30 s for a total of 40 cycles. Relative fold change in VSV P mRNA and anti-genome levels was calculated by ΔΔCt method. Briefly, the difference in threshold cycle (ΔCt) was calculated by dividing Ct value of VSV P mRNA or anti-genome with Ct value of the respective β-actin internal control. The relative fold change in VSV P mRNA or anti-genome levels was calculated by dividing the ΔCt value of siRNA treated sample with ΔCt value of NT siRNA-treated sample.

Semiquantitative RT-PCR. VSV N mRNA and anti-genome levels were examined as described in our previous publication (3).

Cell Viability Measurement. Cell viability was measured by CellTiter Glo assay (Promega). Briefly, 30,000 cells were plated per well in a clear bottom black wall 96-well plate. Cells were treated with the indicated concentrations of the drugs in 100 μL of volume and further incubated for the appropriate length of time. One hundred microliters of CellTiter Glo reagent was added to the wells and incubated at room temperature for 10 min. Readings were taken by using a luminometer.

HIV Pseudotype Experiment. For this experiment, pHIV NL4-3-based, GFP-expressing reporter construct (8) was used. To generate virus stock, 293T cells were cotransfected with an envelope (VSV-G or HIV NL4-3) expressing plasmid, along with an Env-deficient, pHIV NL4-3. HeLa or TZM-bl cells were reverse transfected with siRNAs against COPZ1, COPG, or ATP6V0B. For COPZ1 and COPG transfection, cells were incubated for 28–30 h before infection. For ATP6V0B, cells were incubated for 52 h before infection. The siRNA transfected cells were infected with 1.0×10^5 $TCID_{50}$ VSV-G pseudotyped (HeLa) or NL4-3 env packaged (TZM-bl) virus stock, and GFP-positive cells were measured by flow cytometry (BD FACScan) at 40 hpi. To enhance the infectivity with the NL4-3 env packaged HIV, TZM-bl cells were exposed to DEAE dextran (33.3 μg/mL) simultaneously with virus for 3.5 h. Cells were washed two times with PBS and supplemented with DMEM plus 10% FBS and incubated for 37 h more.

Protein–Protein Interaction Network. Protein–protein interaction network data were downloaded from the STRING Database (9) and manually validated for each interaction. Each network was represented by using the Cytoscape suite (10) as follows: the focal protein for each network (COPA, MAT2A, SCL46A1, and ADAL) and their respective subunits were color-coded and aligned hori-

zontally. Network visualizations were redrawn by centering to these focal proteins and their subunits and to preserve the topologies of most other highly interconnected subnetworks to the highest possible extent.

1. Emonet SF, Garidou L, McGavern DB, de la Torre JC (2009) Generation of recombinant lymphocytic choriomeningitis viruses with trisegmented genomes stably expressing two additional genes of interest. *Proc Natl Acad Sci USA* 106:3473–3478.
2. Zhang L, et al. (2005) Infection of ciliated cells by human parainfluenza virus type 3 in an in vitro model of human airway epithelium. *J Virol* 79:1113–1124.
3. Dinh PX, Beura LK, Panda D, Das A, Pattnaik AK (2011) Antagonistic effects of cellular poly(C) binding proteins on vesicular stomatitis virus gene expression. *J Virol* 85: 9459–9471.
4. Zhang JH, Chung TD, Oldenburg KR (1999) A simple statistical parameter for use in evaluation and validation of high throughput screening assays. *J Biomol Screen* 4:67–73.
5. Snijder B, et al. (2009) Population context determines cell-to-cell variability in endocytosis and virus infection. *Nature* 461:520–523.
6. Barrows NJ, Le Sommer C, Garcia-Blanco MA, Pearson JL (2010) Factors affecting reproducibility between genome-scale siRNA-based screens. *J Biomol Screen* 15: 735–747.
7. Hollander M, Wolfe DA (1999) *Nonparametric Statistical Methods* (Wiley, New York), 2nd Ed.
8. Dapp MJ, Clouser CL, Patterson S, Mansky LM (2009) 5-Azacytidine can induce lethal mutagenesis in human immunodeficiency virus type 1. *J Virol* 83:11950–11958.
9. Szklarczyk D, et al. (2011) The STRING database in 2011: Functional interaction networks of proteins, globally integrated and scored. *Nucleic Acids Res* 39(Database issue):D561–D568.
10. Smoot ME, Ono K, Ruscheinski J, Wang PL, Ideker T (2011) Cytoscape 2.8: New features for data integration and network visualization. *Bioinformatics* 27:431–432.

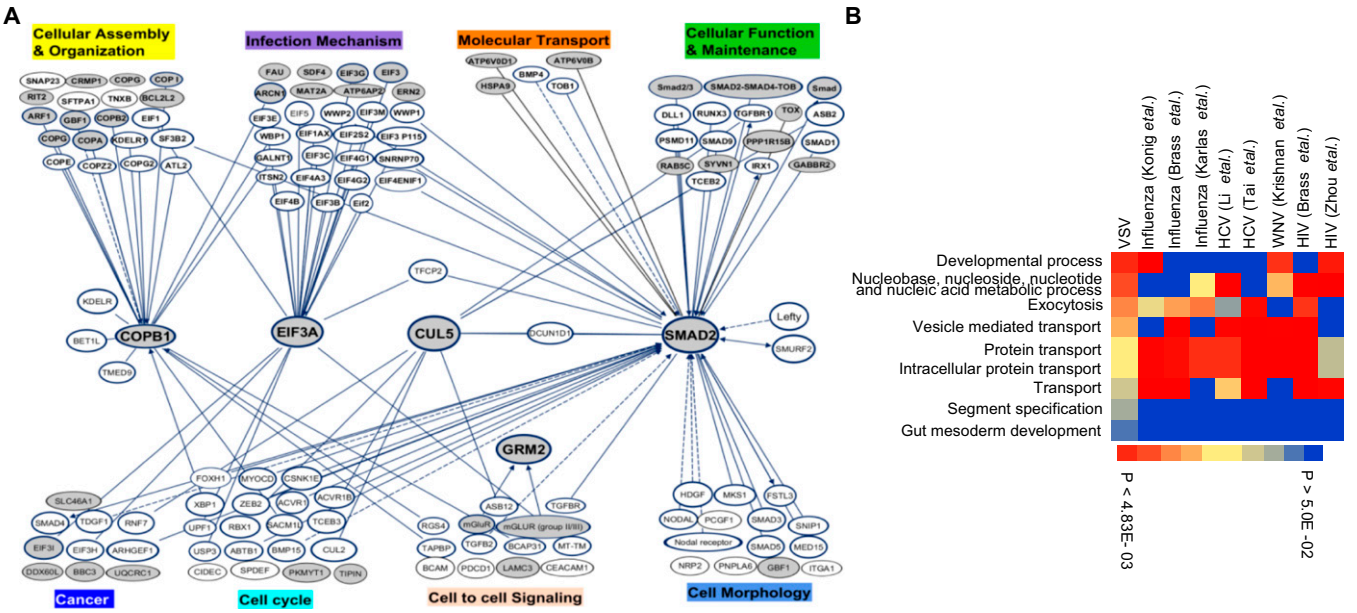

Fig. S1. Computational pathway analysis of identified factors. (*A*) Ingenuity pathway analysis (IPA; Ingenuity Systems) identified 8 top biological functional annotations associated with the 173 identified candidates. Integration of these functions is presented in the form of relationships as direct (solid lines) and indirect (discontinuous lines) interactions with arrows indicating the direction of the underlying relationship when appropriate. The nodes with gray background represent molecules identified in our screen, and those with white background are the molecules forecasted by IPA knowledge base. (*B*) Biological processes enriched among the 72 genes identified in the validation screen for VSV were compared with those identified for other viruses (1–8). Hit lists were accessed from these published articles and subjected to the *Panther* biological classification analysis. The color intensities represent degree of requirement by the indicated virus. Red and gray represent high degree of dependency. Blue represents little or no dependency on the indicated pathway or process.

1. König R, et al. (2010) Human host factors required for influenza virus replication. *Nature* 463:813–817.
2. Brass AL, et al. (2009) The IFITM proteins mediate cellular resistance to influenza A H1N1 virus, West Nile virus, and dengue virus. *Cell* 139:1243–1254.
3. Karlas A, et al. (2010) Genome-wide RNAi screen identifies human host factors crucial for influenza virus replication. *Nature* 463:818–822.
4. Li Q, et al. (2009) A genome-wide genetic screen for host factors required for hepatitis C virus propagation. *Proc Natl Acad Sci USA* 106:16410–16415.
5. Krishnan MN, et al. (2008) RNA interference screen for human genes associated with West Nile virus infection. *Nature* 455:242–245.
6. Brass AL, et al. (2008) Identification of host proteins required for HIV infection through a functional genomic screen. *Science* 319:921–926.
7. Zhou H, et al. (2008) Genome-scale RNAi screen for host factors required for HIV replication. *Cell Host Microbe* 4:495–504.
8. Tai AW, et al. (2009) A functional genomic screen identifies cellular cofactors of hepatitis C virus replication. *Cell Host Microbe* 5:298–307.

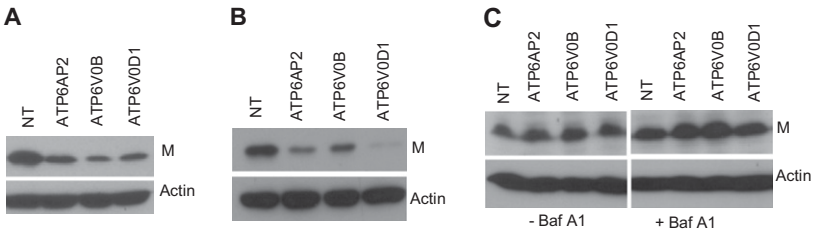

Fig. S2. vATPase is required for VSV infection. (*A*) Cells were transfected with pool of four siRNAs for indicated vATPase subunits for 72 h and infected with VSV (MOI = 0.01) for 14 h. Cell extracts were examined for VSV gene expression (viral M protein) by immunoblotting. Actin is shown for loading control. (*B*) HeLa cells were transfected with the indicated siRNAs and then infected with VSVΔG virus. M protein expression was examined at 5 hpi. (*C*) Cells transfected as above were treated with (+) or without (–) bafilomycin A1 (Baf A1) for 30 min and then transfected with VSV NC. VSV gene expression (M protein) was examined by immunoblotting at 6 h after NC transfection.

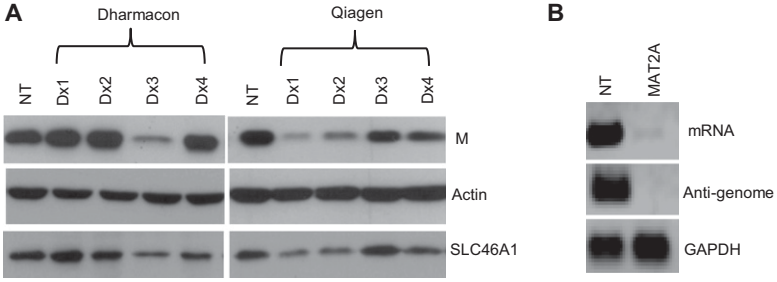

Fig. S3. SLC46A1 and MAT2A are required for VSV infection. (*A*) HeLa cells transfected with individual siRNA duplexes targeting SLC46A1 were subsequently infected with 0.005 MOI of VSV for 14 h. Cell lysates were collected and the viral M protein, actin, and SLC46A1 were examined by immunoblotting. (*B*) HeLa cells were transfected with pool of four siRNAs targeting MAT2A and at 48 hpt were infected with VSV. At 4 hpi, levels of mRNA and antigenomic RNAs were determined as described (1). Levels of glyceraldehyde-3-phosphate dehydrogenase (GAPDH) was shown as internal control.

1. Dinh PX, Beura LK, Panda D, Das A, Pattnaik AK (2011) Antagonistic effects of cellular poly(C) binding proteins on vesicular stomatitis virus gene expression. *J Virol* 85:9459–9471.

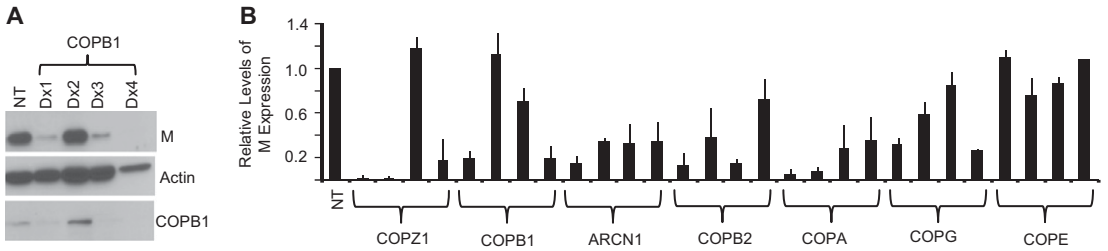

Fig. S4. Effect of depletion of COPI subunits on VSV gene expression. (*A*) HeLa cells transfected with individual siRNA duplexes targeting COPB1 subunit and subsequently were infected with VSV (MOI = 0.5) for 4 h. VSV gene expression was assessed by immunoblotting for M. Depletion of COPB1 was examined by Western blotting. (*B*) HeLa cells transfected with individual siRNA duplexes (four per gene) targeting each of the seven COPI subunits were infected with VSV (MOI = 0.5) for 4 h. VSV gene expression was assessed by immunoblotting for M. Relative levels of M (mean ± SD) from three experiments are presented.

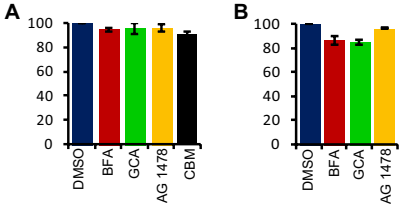

Fig. S5. Cell viability after drug treatment. (*A*) HeLa cells plated in 96-well plate were treated with Brefeldin A (BFA; 5 μg/mL), Golgicide A (10 μM), or AG-1478 (30 μM) for 6 h or CBM (2 mM) for 4 h. Cell viability was measured by CellTiter-Glo assay. (*B*) Cells plated as described in *A* were treated with BFA (200 ng/mL), Golgicide A (5 μM), or AG-1478 (20 μM) for 14 h. Cell viability was measured as described in *A*.

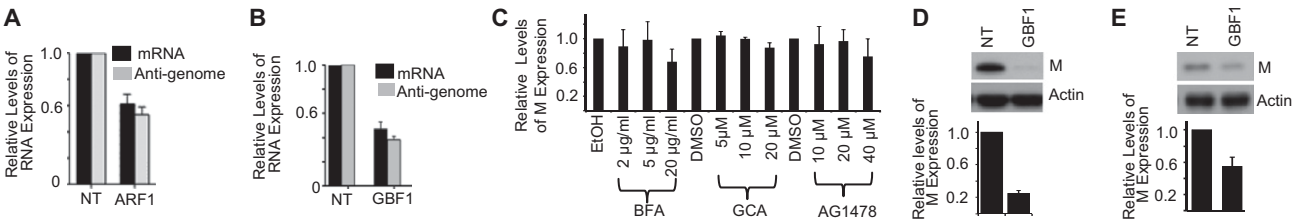

Fig. S6. Disruption of ARF1 and GBF1 functions affects VSV RNA synthesis. (*A* and *B*) HeLa cells were treated with pool of four siRNAs for ARF1 (*A*) or GBF1 (*B*) and then infected with VSV. VSV-P mRNA or anti-genome levels were examined by qRT-PCR. Values show mean ± SE of measurement (SEM) of duplicate reactions from two experiments after normalizing to NT control. (*C*) MDCK cells infected with 1 MOI of VSV were treated with indicated concentrations of the drugs at 1 hpi. Cell lysates were prepared at 4 hpi, and M and actin levels were assessed by immunoblotting. Relative levels of M (mean ± SD) compared with vehicle controls from three experiments are presented. (*D* and *E*) HeLa cells depleted of GBF1 protein by pool of four siRNAs were infected with VSVΔG virus (*D*) or transfected with NCs (*E*). M protein expression was examined at 5 hpi (*D*) or 6 hpt (*E*).

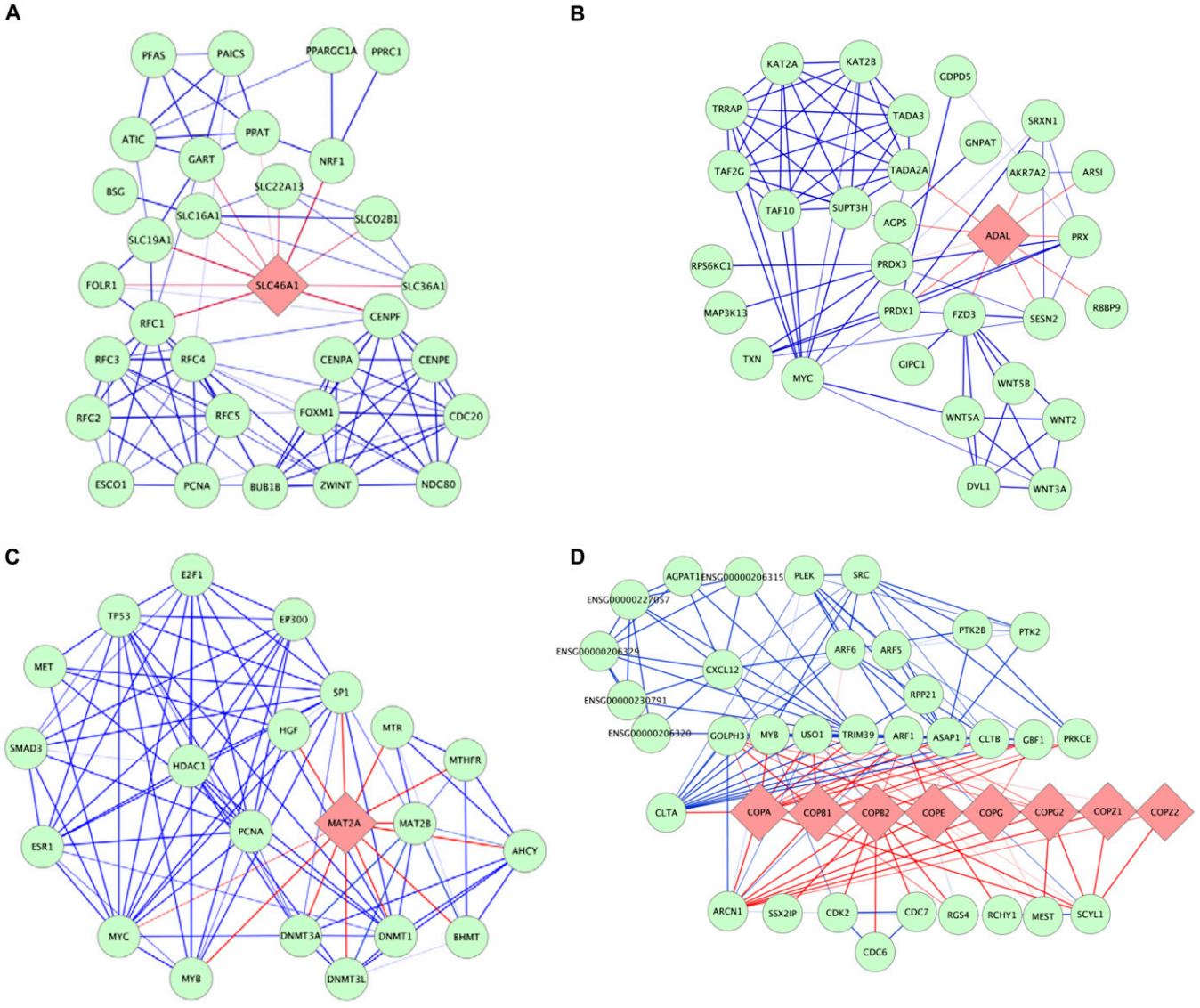

Fig. S7. Protein-protein interaction networks. The protein–protein interaction network for solute carrier family 46, member 1 protein (SLC46A1; proton-coupled folate transporter, PCFT) (*A*), ADAL (*B*), MAT2A (*C*), and COPI (*D*). Edges (interactions) are indicated by red colors. Only the proteins directly interacting with SLC46A1, ADAL, MAT2A, and COPI and their directly interacting proteins are shown. Interactions and annotations were obtained from the STRING Database (1) and from GeneCards (2), and network visualizations were created using Cytoscape (3).

1. Szklarczyk D, et al. (2011) The STRING database in 2011: Functional interaction networks of proteins, globally integrated and scored. *Nucleic Acids Res* 39(Database issue):D561–D568.
2. Safran M, et al. (2010) GeneCards Version 3: The human gene integrator. *Database (Oxford)* 2010:baq020.
3. Smoot ME, Ono K, Ruscheinski J, Wang PL, Ideker T (2011) Cytoscape 2.8: New features for data integration and network visualization. *Bioinformatics* 27:431–432.

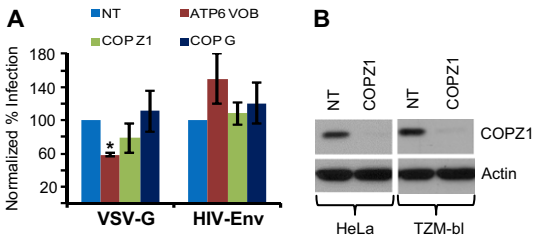

Fig. S8. Depletion of COPI does not affect VSV-G mediated HIV entry. (*A*) COPZ1, COPG, or ATP6V0B siRNAs transfected HeLa cells or TZM-bl cells were infected with VSV-G pseudotyped HIV or NL4-3 env packaged virus, respectively. GFP expressing cells were measured by flow cytometry at 40 hpi. Asterisk indicates statistically significant difference ($P = 0.0001$). (*B*) Depletion of COPZ1 protein was examined by immunoblotting after 24–26 h post siRNA transfection in HeLa and TZM-bl cells.

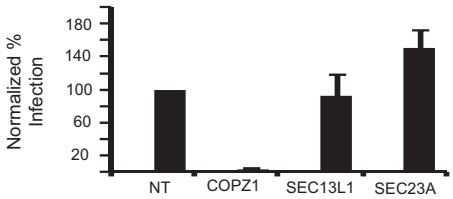

Fig. S9. Transfection of COPII siRNA does not affect VSV infection. HeLa cells were transfected with siRNAs for SEC13L1 and SEC23A (two of the COPII subunits) or against COPZ1. At 48 hpt, cells were infected with VSV (MOI = 0.01), and normalized percent infection relative to NT siRNA at 16 hpi was determined.

Table S1. Primer sequences

Primer	Sequence
VSV 2795F	GTGACGGACGAATGTCTCATAA
VSV2860R	TTTGACTCTCGCCTGATTGTAC
VSV2955R	TGATGAATGGATTGGGATAACA
β-Actin-F	CAAGTACTCCGTGTGTGGAT
β-Actin-R	CATACTCCTGCTTGCTGAT
VSV 2825 probe	6-FAM/CCATCCTGCTCGGCCTGAGATAC/TAMRA
β-Actin probe	Cy5/TCGCTGTCCACCTTCCAGCAGAT/BHQ

Table S2. Primer and probe concentrations

Primer	Primer concentrations, nM	Probe	Probe concentrations, nM
VSV P mRNA			
VSV 2795-F	500	VSV 2825	200
VSV 2860-R	500		
VSV anti-genome			
VSV 2795-F	1,000	VSV 2825	200
VSV 2955-R	1,000		
β-Actin			
β-Actin-F	500	βActin	1,000
β-Actin-R	500		

Dataset S1. List of genes identified in the primary screen for VSV

Dataset S1

Dataset S2. List of genes identified for VSV, VSV/LCMV/HPIV3, VSV/LCMV, or VSV/HPIV3

Dataset S2

Dataset S3. Known and putative biological functions and subcellular localization of genes required for VSV

Dataset S3